Theoretical and Computational Acoustics
D. Lee, Y-H Pao, M.H. Schultz, and Y-C Teng (Editors)

Mode Coupling and Inter-Mode Energy Transfer in Upslope Environments

Timothy H. Ruppel and Robert L. Field
Naval Research Laboratory, Stennis Space Center, MS 39529

The accuracy of the adiabatic approximation is known to be suspect when applied to certain environments, particularly areas along the continental shelf. However, it is often difficult to tell, a priori, if mode coupling is present in a given environment. In an attempt to quantify the degree of mode coupling, the classical mode coupling coefficients are related to energy transfers between modes. As an illustration of this relationship, the coupling coefficients for a rigid bottom, iso-velocity environment with a range-dependent bathymetry were derived analytically. In deriving these coefficients, it was discovered that symmetries in the weak coupling coefficients, which are correct for most other environments, must be modified for the rigid bottom case. The potential for energy transfer was also determined. Simple ratios were derived which may be used to determine the presence and strength of mode coupling in this case. The use of mode coupling coefficients in this way clearly shows when the potential for mode coupling exists, and the coupling strength, if present. An extension to more realistic boundaries is outlined. The method may be used to test the accuracy of other means of predicting the presence or absence of mode coupling, as well as to provide additional useful information, such as the precise modes engaged in coupling.

1 Introduction

When choosing a model for propagation studies or matched field processing, one must often assess the validity of the adiabatic approximation in a given range-dependent environment. Certain propagation models (e.g., ray and adiabatic normal mode models) are computationally fast, but assume no energy transfer between modes, while others allow for mode coupling, but are relatively slow computationally. This paper is a first step toward the development of fast quantitative measures of the validity of the adiabatic approximation which may be easily applied by non-specialists and which are applicable in a wide variety of realistic environments.

One set of numbers which measure the degree of coupling in a given environment is the set of mode coupling coefficients which arises from the propagation physics. The use of these coefficients for the purpose of determining the validity of the adiabatic approximation has a number of advantages: the coefficients describe precisely where mode coupling occurs, they give information on which modes are engaged in coupling, and they may be weighted and summed to provide a single number which may describe the degree of coupling in a given region. Unfortunately, calculating the mode coupling coefficients

can be a computationally intensive task, and the effects of mode coupling may be seen at ranges well past those at which the coupling actually occurs.

The environments under study here are iso-velocity sound speed channels bounded by a range-dependent rigid bottom and a range-independent pressure-release surface; the normal modes and coupling coefficients may be calculated analytically.

In Section 2, the coupling coefficients for the iso-velocity environment will be calculated. Certain symmetries in the weak coupling coefficient which are valid for many environments will be shown to fail here. In Section 3 the propagation physics will be investigated in order to gain insight into the precise relationship between the coupling coefficients and the observed effects of coupling; this relationship is significantly more complex than the term "coupling coefficient" might suggest. Nonetheless, it will be shown that strong coupling is related to an appropriately defined modal potential energy and weak coupling to a modal kinetic energy. In Section 4, simulations will be used to further investigate the use of coupling coefficients as an indicator of mode coupling. Section 5 will contain conclusions and suggestions for further work.

2 Calculation of Coupling Coefficients

The environment under study is described by a constant sound speed c and density ρ, and is bounded below by a rigid surface at range-variable depth $z = H(r)$ and above by a pressure-release surface at $z = 0$. A monochromatic omnidirectional source with frequency ω is located at depth z_s.

A modal decomposition of the velocity potential $\psi(r, z, \omega)$ in terms of local mode eigenfunctions $Z_n(r, z)$ and amplitudes $\varphi_n(r, \omega)$ may be written

$$\psi(r, z, \omega) = \sum_{n=1}^{\infty} \varphi_n(r, \omega) Z_n(r, z) = \sum_{n=1}^{\infty} \psi_n(r, z, \omega), \tag{1}$$

where

$$\psi_n(r, z, \omega) \equiv \varphi_n(r, \omega) Z_n(r, z), \tag{2}$$

and the sums are over the propagating and evanescent modes. The normalization relations for the local modes $Z_n(r, z)$ are

$$\int_0^{H(r)} \rho Z_m(r, z) Z_n(r, z)\, dz = \delta_{mn}. \tag{3}$$

The Helmholtz equation for the region $r > 0$ leads to the coupled mode equations [1,2]

$$\partial_{zz} Z_n(r, z) + [k^2 - k_n^2(\omega)] Z_n(r, z) = 0, \tag{4}$$

$$\left[\partial_{rr} + \frac{1}{r}\partial_r + k_n^2(\omega)\right] \varphi_n(r,\omega) - \sum_{m=1}^{\infty} \left[A_{mn}(r) + B_{mn}(r)\partial_r\right] \varphi_m(r,\omega) = 0, \tag{5}$$

where $k = \omega/c$, $k_n^2(\omega)$ is the mode eigenvalue or horizontal wavenumber, ∂_r indicates the partial derivative with respect to r, ∂_{rr} indicates the second partial derivative with respect to r, and the strong and weak mode coupling coefficients, respectively, are defined by

$$A_{mn}(r) \equiv \int_0^{H(r)} \rho Z_n(r,z) \left[\partial_{rr} + \frac{1}{r}\partial_r\right] Z_m(r,z)\, dz, \tag{6}$$

$$B_{mn}(r) \equiv \int_0^{H(r)} \rho Z_n(r,z) \left[\partial_r Z_m(r,z)\right] dz. \tag{7}$$

The adiabatic approximation is accomplished by setting $A_{mn}(r) = B_{mn}(r) = 0$ for all m, n, and further assuming the WKB approximation. In this paper, it is assumed that the effect of the WKB approximation on the calculated field is negligible.

Under the boundary conditions that $\psi(r,z,\omega)$ vanishes at $z = 0$ and satisfies the Sommerfield radiation condition, and that $\partial_r\psi(r,z,\omega)$ vanishes at $z = H(r)$, the local modes are:

$$Z_n(r,z) = \sqrt{\frac{2}{H(r)}} \sin \frac{\left(n - \frac{1}{2}\right)\pi z}{H(r)} \tag{8}$$

for $0 \le z \le H(r)$. Substituting Eq. 8 into Eqs. 6 and 7 and integrating leads to the mode coupling coefficients:

$$B_{mn}(r) = \begin{cases} \frac{(-1)^{m-n}(2m-1)^2}{2(n-m)(m+n-1)} \frac{H'(r)}{H(r)}, & \text{if } m \neq n, \\ -\frac{H'(r)}{H(r)} & \text{if } m = n, \end{cases} \tag{9}$$

$$A_{mn}(r) = \begin{cases} \frac{B_{mn}(r)}{r} + \frac{(-1)^{m-n}(2m-1)^2}{m^2+n^2-m-n} \\ \quad \times \left[-\frac{H''(r)}{2H(r)} + \left(\frac{3}{2} - \frac{(2n-1)}{m^2+n^2-m-n}\right) \frac{H'^2(r)}{H^2(r)}\right] & \text{if } m \neq n, \\ \left[\frac{13}{4} + \frac{\pi^2\left(n-\frac{1}{2}\right)^2}{3}\right] \left[\frac{H'(r)}{H(r)}\right]^2 - \frac{3}{2}\frac{H''(r)}{H(r)} + \frac{H'(r)}{rH(r)} & \text{if } m = n, \end{cases} \tag{10}$$

where $H'(r) = dH(r)/dr$ and $H''(r) = d^2H(r)/dr^2$.

Under many conditions, Eqs. 3 and 7 lead to the relations $B_{mn}(r) = -B_{nm}(r)$ and $B_{nn}(r) = 0$.[1,3,4,5] These symmetries do not hold for the rigid bottom case. The discrepancy arises since the mode functions in Eq. 8 are non-zero in a depth domain which varies with range. Taking the range derivative of Eq. 3 yields

$$\frac{d}{dr}\left(\int_0^{H(r)} Z_m(r,z)Z_n(r,z)\,dz\right) = \frac{d\delta_{mn}}{dr} = 0.$$

Since the upper limit of the integral is a function of r, Leibniz's rule[6] must be applied to properly interchange the order of differentiation and integration, so that, using Eq. 7:

$$B_{mn}(r) + B_{nm}(r) = -Z_m\left(r, H(r)\right) Z_n\left(r, H(r)\right) H'(r). \tag{11}$$

3 Coupled Modes and Energy

Multiplying Eq. 4 by $\varphi_n(r)$ and Eq. 5 by $Z_n(r,z)$, and summing the results leads to

$$\begin{aligned}\left(\nabla^2 + k_n^2(\omega)\right)\psi_n(r,z,\omega) &= Z_n(r,z)\sum_{m=1}^{\infty}\left[A_{mn}(r) + B_{mn}(r)\partial_r\right]\varphi_m(r,\omega) \\ &\quad +2\partial_r\varphi_n(r,\omega)\partial_r Z_n(r,z) \\ &\quad -\varphi_n(r,\omega)\left[\frac{\partial_r Z_n(r,z)}{r} + \partial_{rr}Z_n(r,z)\right], \end{aligned}\tag{12}$$

where $\psi_n(r,z,\omega)$ is defined in Eq. 2. $\psi_n(r,z,\omega)$ may be expressed as an infinite sum

$$\psi_n(r,z,\omega) = \psi_n^{(0)}(r,z,\omega) + \sum_{m=1}^{\infty}\left[\psi_{mn}^{(S)}(r,z,\omega) + \psi_{mn}^{(W)}(r,z,\omega)\right], \tag{13}$$

such that

$$\begin{aligned}\left(\nabla^2 + k_n^2(\omega)\right)\psi_n^{(0)}(r,z,\omega) &= -\varphi_n(r,\omega)\left[\frac{\partial_r Z_n(r,z)}{r}\partial_{rr}Z_n(r,z)\right] \\ &\quad +2\partial_r\varphi_n(r,\omega)\partial_r Z_n(r,z), \end{aligned}\tag{14}$$

$$\left(\nabla^2 + k_n^2(\omega)\right)\psi_{mn}^{(S)}(r,z,\omega) = A_{mn}(r)Z_n(r,z)\varphi_m(r,\omega), \tag{15}$$

$$\left(\nabla^2 + k_n^2(\omega)\right)\psi_{mn}^{(W)}(r,z,\omega) = B_{mn}(r)Z_n(r,z)\partial_r\varphi_m(r,\omega). \tag{16}$$

The boundary conditions on $\psi_n^{(0)}$, $\psi_{mn}^{(S)}$, and $\psi_{mn}^{(W)}$ are the same as those for ψ_n.

The partition of $\psi_n(r,z,\omega)$ was achieved so that the effects of strong and weak coupling from each mode can be easily identified. The single uncoupled equation Eq. 14 is seen to be Eq. 12 with $A_{mn}(r) = B_{mn}(r) = 0$, so that $\psi_n^{(0)}(r,z,\omega)$ is the velocity potential obtained under the adiabatic approximation without the WKB approximation. The set of equations Eq. 15 each have a right hand side multiplied by $A_{mn}(r)$ so that $\psi_{mn}^{(S)}(r,z,\omega)$ represents the change in $\psi_n(r,z,\omega)$ due to strong coupling from mode m. Similarly, the form of the set of equations Eq. 16 implies that $\psi_{mn}^{(W)}(r,z,\omega)$ represents the change in $\psi_n(r,z,\omega)$ due to weak coupling from mode m. Note that Eqs. 14 – 16 still represent coupled equations; they were not derived as an improvement over Eqs. 4 and 5 in calculating the field. However, Eqs. 15 and 16 are of the form of Helmholtz equations where the terms on the right hand sides represent distributed sources.

The right hand side of Eqs. 15 and 16 may be expanded into an infinite collection of vertical line sources. That is, the coupling into mode n from mode m at range r can be seen to be due to vertical line sources with strengths $A_{mn}(r)Z_n(r,z)\varphi_m(r,\omega)/4\pi$ and $B_{mn}(r)Z_n(r,z)\partial_r\varphi_m(r,\omega)/4\pi$. By calculating the farfield time-averaged power output from each of these sources, the effect of any coupling which occurs at range r will be determined, and then related to the total kinetic and potential energy in the mode m.

Consider first the strong coupling equations Eq. 15. The solution of this equation with the given boundary conditions is difficult, even in the case where $A_{mn}(r) = A'_{mn}\delta(r-r')$, i.e., where the right hand side specifies a line source. The proper solution would take into account the effects on $\psi_{mn}^{(S)}$ of bathymetry changes far removed from r'. This detracts from the goal of determining the degree of coupling at range r' independent of the rest of the environment. We therefore calculate not $\psi_{mn}^{(S)}$ but the value $\xi_{mn}^{(S)}$ which is the solution of Eq. 15 in the free-field, which may be calculated by separation of variables: [7]

$$\begin{aligned}\xi_{mn}^{(S)}(r,z,\omega) &= \frac{A_{mn}(r')\varphi_m(r')Z_n(r',z)}{4\pi} H_0^{(1)}[(r-r')k_n] \\ &\underset{r\to\infty}{\longrightarrow} \frac{A_{mn}(r')\varphi_m(r',\omega)Z_n(r',z)}{\sqrt{8\pi^3(r-r')k_n(\omega)}} e^{i[k_n(\omega)(r-r')-\pi/4]}, \quad (17)\end{aligned}$$

where $H_0^{(1)}(r)$ is the zeroth order Hankel function of the first kind, and the $Z_n(r',z)$ are defined in Eq. 1. This is a free-field solution which, it can be argued, ignores the very thing which gave rise to the coupling in the first place, i.e., a range-variable boundary condition. However, it is one purpose of

this calculation to attempt to isolate the effects of coupling at range r from those at a different range r'.

The time-averaged far-field power output may be calculated:

$$\begin{aligned} P_{mn}^{(S)}(r',\omega) &= 2\pi \int_0^{H(r')} (r-r') \left[\mathbf{I}_{mn}^{(S)}(r,z,\omega) \cdot \hat{\mathbf{r}} \right] dz \\ &= -2\pi i\omega\rho \int_0^{H(r')} (r-r') \left\langle \xi_{mn}^{(S)}(r,z,\omega) \nabla \xi_{mn}^{(S)}(r,z,\omega) \cdot \hat{\mathbf{r}} \right\rangle dz \\ &= \frac{\omega}{4\pi^2} [A_{mn}(r')]^2 |\varphi_m(r',\omega)|^2, \end{aligned} \tag{18}$$

where $\langle \cdots \rangle$ represents the time average, $\hat{\mathbf{r}}$ is a unit vector pointing toward positive r, and $\mathbf{I}_{mn}^{(S)}(r,z,\omega)$ is the time-averaged far-field intensity. The integral over depth was calculated using Eq. 3.

The *modal potential energy* $V_m(r,\omega)$ will be defined as the total potential energy at some range r which the field would have if the mode m were the only mode excited. Using the standard equation for potential energy: [8]

$$\begin{aligned} V_m(r,\omega) &\equiv \frac{1}{2\rho c} \int_0^{H(r)} |p_m(r,z,\omega)|^2 \, dz = \frac{\omega^2}{2c} \int_0^{H(r)} \rho \, |\psi_m(r,z,\omega)|^2 \, dz \\ &= \frac{\omega^2}{2c} |\varphi_n(r,\omega)|^2 . \end{aligned} \tag{19}$$

Therefore, comparing Eq. 19 and Eq. 18, gives the relation

$$P_{mn}^{(S)}(r',\omega) = \frac{c}{2\pi^2\omega} A_{mn}^2(r') V_m(r',\omega). \tag{20}$$

Next, consider Eq. 16, the weak coupling equations. The time-averaged far-field power output, due to a line source at $r = r'$ in a free-field environment with strength $B_{mn}(r')Z_n(r,z)\partial_r\varphi_m(r,\omega)/4\pi$, is

$$P_{mn}^{(W)}(r',\omega) = \frac{\omega}{4\pi^2} |B_{mn}(r')|^2 \, |\partial_r \varphi_m(r',\omega)|^2 . \tag{21}$$

The *modal kinetic energy* $T_m(r,\omega)$ will be defined in a manner similar to the modal potential energy, i.e., the total kinetic energy at some range r which the field would have if the mode m were the only mode excited. Using the standard equation for kinetic energy: [8]

$$
\begin{aligned}
T_m(r,\omega) &\equiv \frac{1}{2}\int_0^{H(r)} \rho\,|\mathbf{v}_m(r,z,\omega)|^2\,dz \\
&= \frac{1}{2}\int_0^{H(r)} \rho\,|\nabla\psi_m(r,z,\omega)|^2\,dz \\
&= \frac{1}{2}\Bigg\{[\partial_r\varphi_m(r,\omega)]^2\int_0^{H(r)}\rho\,[Z_m(r,z)]^2\,dz \\
&\quad + [\varphi_m(r,\omega)]^2\int_0^{H(r)}\rho\left([\partial_r Z_m(r,z)]^2 + [\partial_z Z_m(r,z)]^2\right)dz \\
&\quad + \varphi_m(r,\omega)\partial_r\varphi_m(r)\int_0^{H(r)}\rho Z_m(r,z)\partial_r Z_m(r,z)\,dz\Bigg\}. \qquad (22)
\end{aligned}
$$

With some manipulation, including the use of Eq. 3, Eqs. 6 – 10, and Leibniz's rule, one obtains

$$
T_m(r,\omega) = \frac{[\partial_r\varphi_m(r,\omega)]^2}{2} + \frac{T'_m(r)}{2}\varphi_m^2(r,\omega) - \varphi_m(r,\omega)\partial_r\varphi_m(r,\omega)\frac{H'(r)}{2H(r)}, \qquad (23)
$$

where

$$
\begin{aligned}
T'_m(r) &= -\frac{H''(r)}{4H(r)} + \frac{H'(r)}{H(r)}\left[1-\frac{2}{r}\right] - \left[\frac{H'(r)}{H(r)}\right]^2\left[\frac{13}{4}+(-1)^m\right] \\
&\quad + \frac{\pi^2\left(m-\frac{1}{2}\right)^2}{H^2(r)}\left[\rho - \frac{[H'(r)]^2}{3}\right].
\end{aligned}
$$

The first term in Eq. 23 is proportional to $P_{mn}^{(W)}(r',\omega)$. Also, note that $T'_m(r)$ increases with increasing m so that the ratio

$$
\tau_m(r',\omega) = \frac{|\partial_r\varphi_m(r')|^2}{T_m(r')} \qquad (24)
$$

is an environment-dependent function which, all else being equal, tends to decrease with increasing mode number. Eq. 21 may be written

$$
P_{mn}^{(S)}(r',\omega) = |B_{mn}(r')|^2\,\tau_m(r',\omega)T_m(r',\omega). \qquad (25)
$$

The degree of strong coupling is therefore, according to Eq. 20, related to the potential energy of the individual modes, while weak coupling, according to Eq. 25, is related to the kinetic energy of the individual modes.

Aside from any qualitative understanding of mode coupling Eqs. 20 and 25 may provide, certain quantitative predictions may also be made. The general decrease in $\tau_m(r)$ with increasing m indicates that the effects of weak mode coupling should decrease with increasing mode number, even if the weak coupling coefficients themselves are identical. The dependence of $P_{mn}^{(S)}(r)$ on ω and c indicate that the effects of strong coupling should decrease with increasing frequency or decreasing sound speed, even though the coupling coefficient is independent of frequency. Also, if something is known about the distribution of potential and kinetic energy in the sound field, the relative effects of strong and weak coupling can perhaps be better understood.

4 Simulations

In this section, the dependence of weak coupling on mode number will be tested using simulations. Strong coupling will not be investigated here; the strong coupling coefficients are usually much smaller than the weak coupling coefficients, with the somewhat surprising result that the effects of "strong" coupling are usually quite small.[9,10] The sound field was modeled using Porter's **KRAKEN** normal mode program,[11] which allows for a perfectly rigid bottom and may be run either using adiabatic or one-way coupled modes with nearly identical input files.

Since the weak coupling coefficients given in Eq. 9 are directly dependent on the factor $H'(r)/H(r)$, then setting the bottom depth equal to an exponential function of range, $H(r) = H_0 e^{-\gamma r}$, where H_0 and γ are appropriately chosen constants, will produce a non-zero, constant weak coupling coefficient. (Also note that Eq. 10 indicates that the strong coupling coefficients will also be of the form of a constant plus a $1/r$ term.) In order to minimize nearfield effects at the receiver, the bathymetry used here has the form

$$H(r) = \begin{cases} H_0 & \text{if } r < r_0, \\ H_0 e^{-\gamma(r-r_0)} & \text{if } r > r_0. \end{cases} \tag{26}$$

The coupling coefficients are identically zero in the region $r < r_0$.

The frequency f and initial depth H_0 were chosen so that a fairly small number of propagating modes exist, thereby reducing processing time and storage requirements. With $f = 100$Hz and $H_0 = 200$ m, 27 modes exist in the region $r \leq r_0$. The coupling coefficients B_{mn} (and therefore γ) must be chosen small enough to allow the sound to propagate, but large enough for the coupling effects to be significant. The relationship between B_{mn} and γ may

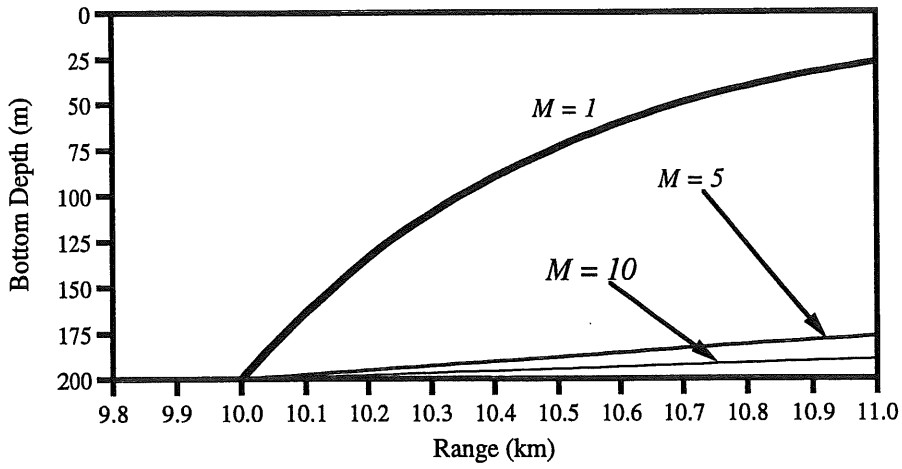

Figure 1: Rigid bottom, iso-velocity test bathymetries with constant weak coupling coefficients. In each case, $B_{M\,(M+1)} = 0.1$ at ranges between 10 and 11 km in range, and zero at ranges less than 10 km.

be determined from Eq. 9:

$$\gamma = \frac{2B_{mn}}{H_0}\left|\frac{(n-m)(n+m-1)}{(2m-1)^2}\right|. \tag{27}$$

Model runs on a range-independent environment with depth H_0 show that $r_0 = 10$ km should be more than sufficient. $H(r)$ was therefore defined in the region $0 < r < 11$ km, with $r_0 = 10$ km.

A set of environments with bathymetries described by Eq. 26 were chosen, each with a "featured mode" M. The depth decay constant γ for each environment was chosen such that $B_{M\,(M+1)} = 0.1$. The bathymetries for the environments with $M = 1, 5, 10$ are plotted in Figure 1.

In addition, each environment was ensonified with 27 sources (coinciding with the number of propagating modes at $r \leq r_0$) spanning the 200 m water channel. The sources were weighted in order to excite the featured mode and only that mode. This was achieved by using LU decomposition [12] to solve for $\mathbf{W}$ in the matrix equation

$$\mathbf{\Psi}(r,\omega) = \mathbf{\Phi}(r,\omega)\mathbf{W}(r,\omega), \tag{28}$$

where $\Psi_j = \delta_{jM}$ is the mode amplitude of the jth mode at the range r, Φ_{ij} is the mode amplitude of the jth mode due to the ith source, and W_i is the

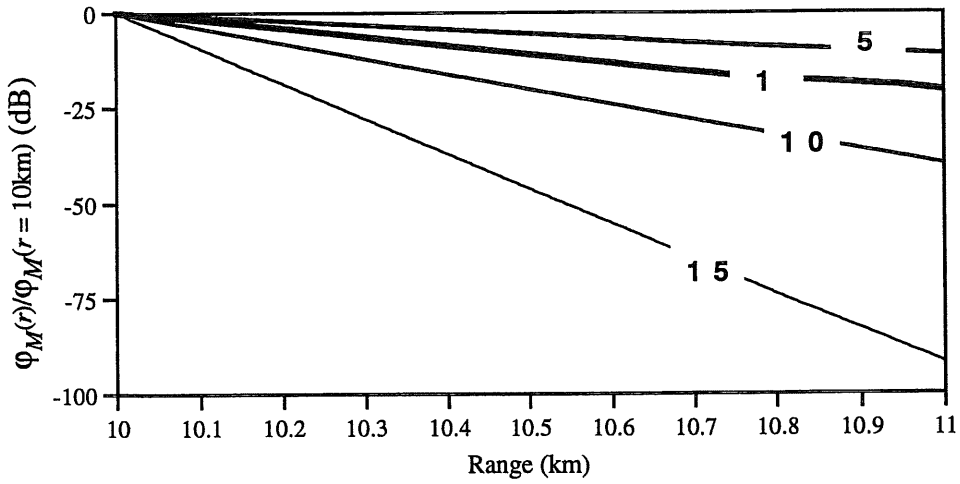

Figure 2: Featured mode amplitudes as a function of range relative to the amplitude at $r = 10$ km for four environments . Adiabatic normal mode theory predicts a loss of approximately 0.5 dB/km.

weight applied to the ith source. Eq. 28 was solved with $r = 1$ m, and ω corresponding to 100 Hz. In all cases, the mode amplitudes for modes $m \neq M$ at $r = 1$ m were more than 50 dB down from the mode M amplitude and, in the vast majority of cases, these modes were more than 125 dB down.

Figure 2 shows the absolute value of the featured mode amplitudes in their respective environments for $M = 1, 5, 10, 15$. Plotted are the ratios $\varphi_M(r)/\varphi_M(r = 10 \text{ km})$ expressed in dB. Note that each featured mode amplitude decreases at a rate much faster than the roughly 0.5 dB/km predicted by adiabatic normal mode theory. However, the change is less pronounced (and the propagation therefore "more adiabatic") in the $M = 5$ conditions than in the $M = 1$ conditions, and more pronounced (and the environment therefore "more coupled") in the $M = 10$ and $M = 15$ conditions.

To further investigate this phenomenon, Figure 3 summarizes the data from a larger set of conditions by displaying the ratio $\varphi_M(r = 11 \text{ km})/\varphi_M(r = 10 \text{ km})$, expressed in dB, where $\varphi_M(r)$ was calculated in the environment where $B_{M(M+1)} = 0.1$. While this ratio decreases over the first three modes, indicating more adiabatic propagation, the difference increases for $M > 3$, indicating more coupled propagation.

The featured mode kinetic energies for $M = 1, 5, 10, 15$ (calculated from Eq. 23) are plotted as a function of range in Figure 4. All modal kinetic energies are plotted relative to $T_1(r = 10 \text{ km})$ in the $M = 1$ environment

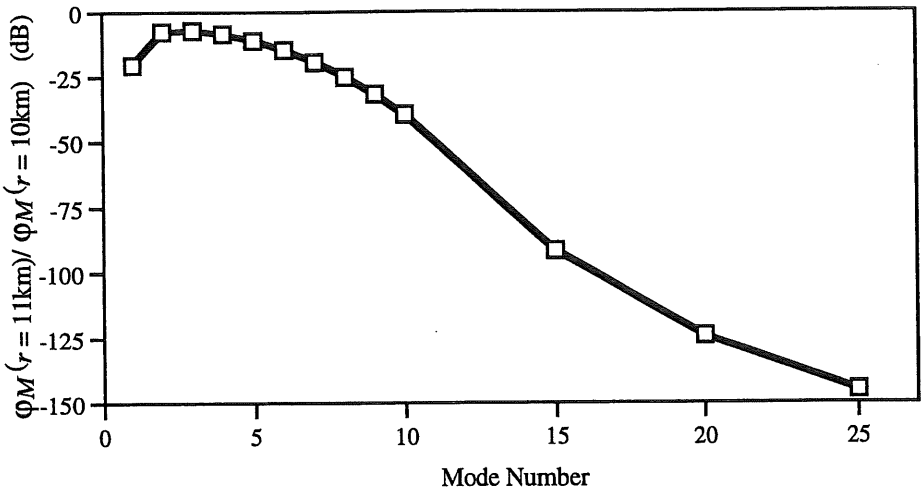

Figure 3: Featured mode amplitudes at $r = 11$ km relative to the amplitude at $r = 10$ km for 13 different environments.

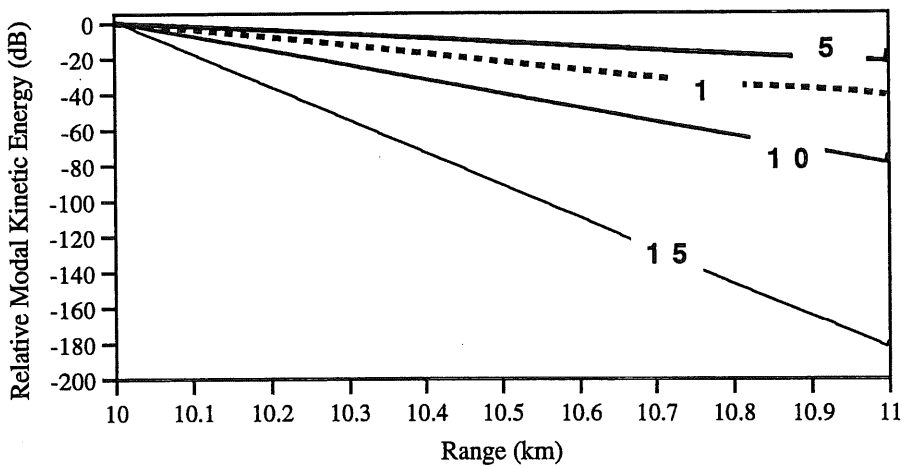

Figure 4: Featured mode kinetic energies (calculated from Eq. 23 as a function of range for $M = 1, 5, 10, 15$.) Plotted values are relative to $T_1(r = 10$ km) in the $M = 1$ environment.

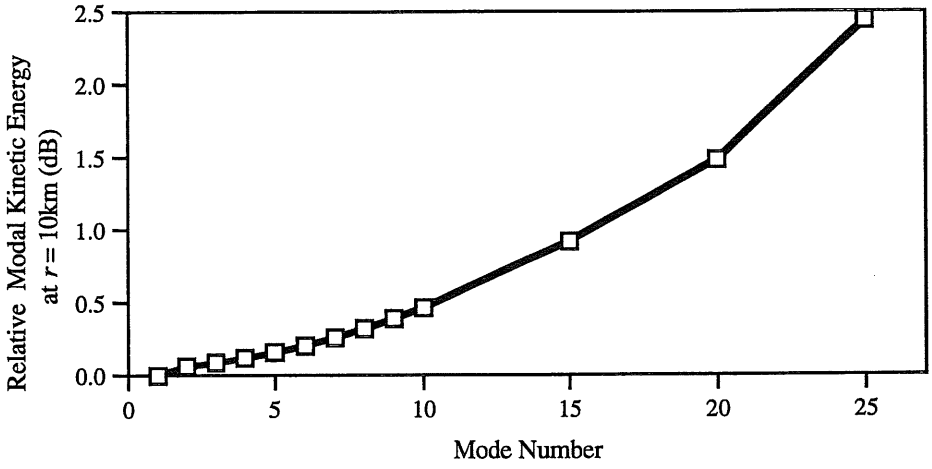

Figure 5: Featured mode kinetic energies at $r = 10$ km relative to the value for $M = 1$.

(where $B_{12} = 0.1$). Concurrent with the decrease in coupling exhibited in Figure 2 between the $M = 1$ and $M = 5$ environments, there is also a decrease in the slope of the featured mode's kinetic energy as a function of range.

Figure 5 shows the initial ($r = 10$ km) modal kinetic energies for the featured modes in their respective environments. It is clear from the chart that the featured mode kinetic energies at $r = 10$ km is an increasing function of mode number. The change in $T_M(r = 10 \text{ km})$ is far less dramatic than the change in the featured mode kinetic energies over the run of the slope. Figure 6 charts the ratio of $T_M(r = 11 \text{ km})/T_M(r = 10 \text{ km})$ (expressed in dB) for the featured modes as a function of mode number. Since the dependence of the modal amplitude on range in the upslope area was exponential (see Figure 2) it is perhaps no surprise that the tendencies shown in Figure 6 are similar to those in Figure 3, that is, both featured mode amplitude and featured mode kinetic energy diminish more slowly in the first three environments, and more quickly in the remaining environments.

The ratio $\tau_m(r, \omega)$, defined in Eq. 24, is nearly constant with respect to range for the featured modes in each environment studied. Figure 7 shows the value of $\tau_m(r = 10 \text{ km})$ for several environments. As expected, this ratio decreases with mode number.

In short, the similarities between Figures 3 and 6 and between Figures 2 and 4 tend to indicate that weak mode coupling and modal kinetic energy are strongly linked, as predicted in theory. Also, the decrease in $\tau_M(r)$ with

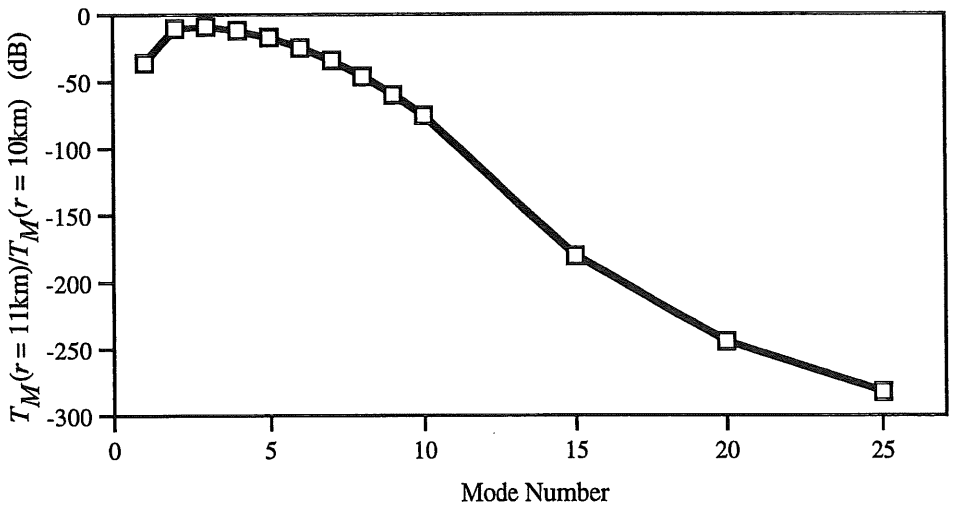

Figure 6: Change in featured mode kinetic energies, from $r = 10$ km to $r = 11$ km, as a function of featured mode number.

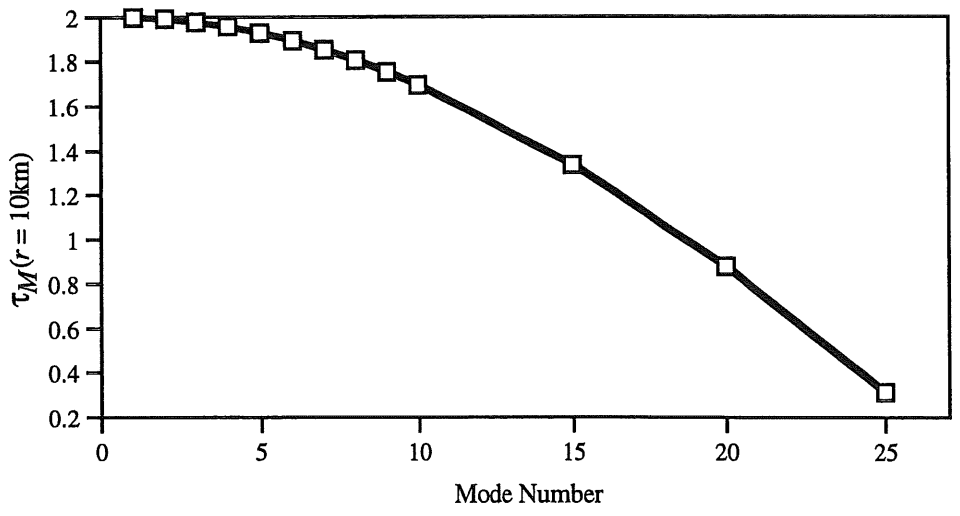

Figure 7: The value of $\tau_m(r = 10$ km) for the featured modes in their environments.

increasing M, predicted in Section 3, is validated in Figure 7. Based on the analysis in Section 3, and the observed behavior of $\tau_M(r)$, one might conclude that the trend toward adiabatic propagation begun in the first three environments in Figures 3 and 6 would continue into higher mode numbers M. The fact that it does not may be due to coupling between mode M and mode $M-1$. Eq. 9 shows that $\left|B_{M\,(M+1)}/B_{M\,(M-1)}\right| = 1-(1/M)$, so that at higher modes more coupling "down" to lower modes is expected. There may also be other effects, as yet not understood, which precipitate the rapid decrease in kinetic energy, and increase in coupling, with increasing featured mode number. Further investigation is required to reveal the exact mechanisms involved.

5 Conclusions

Many theoretical discoveries were made in this research. In Section 2, the weak and strong coupling coefficients for a rigid bottom iso-velocity environment were calculated, and the results were shown to depend on the ratios $H'(r)/H(r)$ and $H''(r)/H(r)$, where $H(r)$ is the bottom depth as a function of r, and $H'(r)$ and $H''(r)$ were the first and second range derivatives of $H(r)$. The relationship between the weak mode coupling coefficients (i.e., $B_{mn} = -B_{nm}$) was shown not to hold in an iso-velocity rigid bottom environment .

In Section 3, weak mode coupling was associated with a "modal kinetic energy," (i.e., the kinetic energy which would be present if only a single mode were excited). Likewise, strong mode coupling was associated with a "modal potential energy."

The theory in Section 3 above must be improved for quantitative predictions to be made. The theory must be extended, perhaps by doing away with the free-field approximations to the radiated power in Eqs. 18 and 21, and certainly by inclusion of more general environments.

The purpose of this research is to develop aids for the matched field processor or other propagation modeler to better determine when coupled mode models are necessary. It is clear, from the simulations in Section 4, that simply describing a single coupling coefficient does not provide this service, since the effects of coupling on mode amplitude etc. may vary widely, even if the coupling coefficient to the nearest neighbor mode is kept constant. With some additional information, however, it may be possible to provide the user with the information he requires.

Acknowledgments

Work supported by the Office of Naval Research Program Element 602435, with technical management provided by the Naval Research Laboratory.

References

1. Allan D. Pierce. Extension of the method of normal modes to sound propagation in an almost-stratified medium. *J. Acoust. Soc. Am.*, 37(1):19–27, January 1965.
2. D. Michael Milder. Ray and wave invariants for sofar channel propagation. *J. Acoust. Soc. Am.*, 46(5):1259–63, November 1969.
3. Leif Abrahamson and Heinz-Otto Kreiss. Numerical solution of the coupled mode equations in duct acoustics. *J. of Comp. Phys.*, 111:1–14, 1994.
4. Finn B. Jensen, William A. Kuperman, Michael B. Porter, and Henrik Schmidt. *Computational Ocean Acoustics.* AIP Series in Modern Acoustics and Signal Processing. AIP Press, New York, 1994.
5. Gregory Gillette. Coupled modes in a waveguide with a range-dependent rigid basement. *J. Acoust. Soc. Am.*, 95(1):187–200, January 1994.
6. Mary L. Boas. *Mathematical Methods in the Physical Sciences.* John Wiley and Sons, New York, 2nd edition, 1983.
7. Philip McCord Morse and K. Uno Ingard. *Theoretical acoustics.* International series in pure and applied physics. McGraw-Hill, New York, 1968.
8. Allan D. Pierce. *Acoustics: An Introduction to Its Physical Principles and Applications.* The Acoustical Society of America, Woodbury, NY, 1989.
9. Steven R. Rutherford and Kenneth E. Hawker. An examination of the influence of the range dependence of the ocean bottom on the adiabatic approximation. *J. Acoust. Soc. Am.*, 66(4):1145–51, October 1979.
10. Steven R. Rutherford and Kenneth E. Hawker. Consistent coupled mode theory of sound propagation for a class of nonseperable problems. *J. Acoust. Soc. Am.*, 70(2):554–564, August 1981.
11. Michael B. Porter. The kraken normal mode program. SACLANTCEN Memorandum SM-245, SACLANT Undersea Research Center, San Bartolomeo, Italy, September 1991.
12. William H. Press, Saul A. Teukolsky, William T. Vetterling, and Brian P. Flannery. *Numerical Recipes in C: The Art of Scientific Computing.* Campridge University Press, Cambridge, England, 2nd edition, 1992.